EFFECTS OF ANTIMONY SURFACTANT ON INDIUM GALLIUM NITRIDE GROWN BY ORGANOMETALLIC VAPOR PHASE EPITAXY

by

Jason Lawrence Merrell

A thesis submitted to the faculty of
The University of Utah
in partial fulfillment of the requirements for the degree of

Master of Science

Department of Materials Science and Engineering

The University of Utah

December 2012

The University of Utah Graduate School

STATEMENT OF THESIS APPROVAL

The thesis of **Jason Lawrence Merrell**

has been approved by the following supervisory committee members:

Feng Liu	, Chair	**10/24/2012** Date Approved
Gerald B. Stringfellow	, Member	**10/24/2012** Date Approved
Ashutosh Tiwari	, Member	**10/24/2012** Date Approved

and by **Feng Liu** , Chair of

the Department of **Materials Science and Engineering**

and by Charles A. Wight, Dean of The Graduate School.

ABSTRACT

This work reviews the fundamentals of InGaN materials and of surfactant effects in surfactant-mediated heteroepitaxial growth. The basic surface processes and possible surfactant mechanisms are presented. These principles are then applied to a study of the effects of Sb surfactant on InGaN grown by organometallic vapor phase epitaxy (OMVPE). Eight samples of InGaN were prepared with varying amounts of Sb (0-2.5%) present during growth. The samples were characterized by atomic force microscopy (AFM), photoluminescence (PL), near field scanning optical microscopy (NSOM), scanning electron microscopy (SEM), and scanning transmission electron microscopy (STEM). InGaN grown without surfactant was smooth with large, wide islands and low island density. Samples grown with 0.5%, 0.75%, and 1% Sb showed an increase in 3D island growth and displayed a blue PL emission peak (~460 nm). STEM showed an In-rich InGaN film with three dimensional (3D) islanding or quantum dots (QDs) on the surface. Samples grown with 1.25%, 1.75%, 2% and 2.5% Sb showed a drastic increase in 3D island density. These samples showed a green (~550 nm) emission peak. STEM showed a different In distribution, with In-rich QDs on the surface. The sudden change in surface morphology and PL emission peak suggest that Sb induces a different surface reconstruction at a certain threshold concentration between 1% and 1.25% that affects In incorporation or In distribution in the film as well as overall surface morphology.

TABLE OF CONTENTS

LIST OF FIGURES

ACKNOWLEDGEMENTS

First of all I would like to thank my advisor, Dr. Feng Liu. He has been a great teacher and mentor to me over the past few years and I will benefit greatly from my interaction with him. I would also like to thank Dr. Gerald Stringfellow for his time and instruction over the past two years.

I also thank Dr. Densen Cao of CAO Group Inc. for providing the InGaN samples and project funding. This work would not have happened without his contribution. Thanks are also extended to Sebastian Bange for insightful technical discussions, Brian van Devener of the Micron Microscopy Core at the University of Utah for help with AFM imaging, and Randy Polson of the Dixon Laser Institute at the University of Utah for the PL measurements.

Last but not least I would like to thank my wife, Michelle, for her love, support, and patients throughout my entire academic career.

INTRODUCTION

InGaN has become a topic of intense research due to its invaluable optoelectronic properties. This ternary III/V semiconductor is a seemingly ideal material for LEDs due to its direct bandgap that is tunable across the visible range by varying the relative amounts of GaN and InN. InGaN is currently used in commercially produced blue and green LEDs, but the material makes poor yellow and red LEDs due to inherent materials quality issues. AlInGaN and related alloys are also of great interest in high frequency, high power devices due to their good mechanical and thermal stability. The alloy system could also be of great use in multi-junction solar cells because one material system could achieve all of the different bandgaps required for efficiency.

InGaN is a combination of two binary compounds, GaN and InN. These members of the polymorphic III/V nitride family (which include GaN, InN, and AlN) can crystallize in the wurtzite and zincblende crystal structures. The wurtzite polymorph, a common structure for binary compounds, is a hexagonal close packed (HCP) structure with atoms having tetrahedral coordination (Figure 1). The two different atom types in the binary compound form two interpenetrating HCP sublattices. This creates a material with piezoelectric properties due to the lack of inversion symmetry in the lattice, as illustrated by the wurtzite unit cell in Figure 1. The zincblende structure has similar tetrahedral coordination but the two atom types in a binary compound form two interpenetrating face-centered cubic (FCC) lattices (Figure 2). When InN is added to GaN to form InGaN, the In substitutes for the Ga on the group III sublattice. Due to the symmetry of the zincblende polymorph, it does not exhibit the same piezoelectric properties.

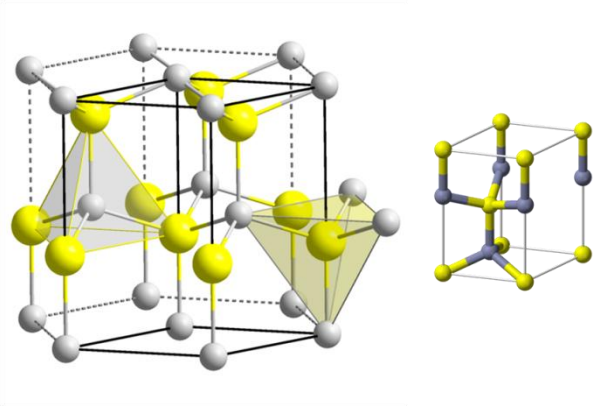

Figure 1 The wurtzite crystal structure of GaN and its unit cell.

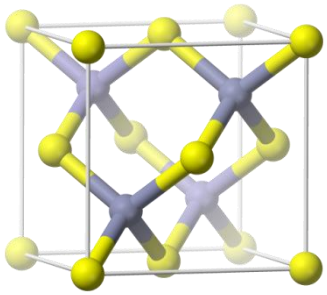

Figure 2 The zincblende crystal structure of GaN.

Although this material is in wide use as the active layer in many optoelectronic devices, the fundamental physics of this material has not yet been well developed. Some of its physical and chemical properties are estimated from the separate binary materials.[1] Vegard's Law is commonly used to estimate the lattice parameter of InGaN based on the properties of GaN and InN. This approximate, empirical rule dictates that a linear relationship holds between the lattice parameter of an alloy and the concentration of its constituent elements. This relationship also holds for calculating the bandgap energy when used in conjunction with a bowing parameter. This takes into account the nonlinear effects of alloying by quantifying the deviation from linearity. However, due to effects such as strain, inhomogeneity, phase separation, and measuring techniques, a range of bowing parameters have been reported. This has complicated the study of InGaN, despite the fact that much progress has recently been made with this material.

Challenges of Epitaxial Growth of III/Vs

Epitaxial growth of nitride semiconductors has also been challenging and difficult to understand. This can be attributed to many materials problems: lack of a native substrate and lattice mismatch, solid phase miscibility gap between GaN and InN, comparatively high vapor pressure of InN, and difference in formation enthalpies of GaN and InN. These problems all contribute to material defects, inhomogeneous alloying, and heterostructures in and on the material that affect the emission characteristics. InGaN is usually grown on sapphire or SiC with a buffer layer of GaN. The difference in crystal lattice and thermal expansion between the substrate and film creates a high density of threading dislocations and defects in the film despite the use of the buffer layer. The result is an epitaxial film with twins, stacking faults, interface defects, and a dislocation density of 10^{8}-10^{10} cm^{-2}.[1] Most other materials would be rendered

useless as light emitters due to this high dislocation density but InGaN remains efficient, probably due to its microstructure. It has been theorized that a quantum well effect occurs where compositional fluctuations in the alloy localize charge carriers for radiative recombination before they reach dislocations that cause nonradiative recombination.[1] Other materials issues arise because epitaxial InGaN is strained due to the lattice mismatch of GaN and InN. The strain causes Stranski-Krastanov growth in which a thin wetting layer is deposited, followed by formation of small islands with high surface coverage density. Strain during epitaxial growth has also led to the formation of v-defects that propagate upward from the interface to the surface of the film in order to relax strain.[2] These are usually seen when InGaN/GaN multiquantum wells are grown for use in light emitters.[3]

The problem that arises from the high relative vapor pressure of InN is low indium incorporation in the solid due to In surface desorption. Surface desorption can be reduced by decreasing the OMVPE growth temperature but this also decreases the cracking efficiency of ammonia which leads to a slower growth rate that could decrease the amount of In incorporation into the film. Both of these phenomena increase the concentration of In diffusing on the surface so growth parameters have to be optimized in order to avoid forming In droplets on the surface. This problem is also related to the problem that arises from the large difference in formation enthalpy of the GaN and InN. GaN (ΔH_f=-158kJ/mol) forms much more favorably than InN, further hindering InN incorporation into the film.

The problem of phase separation by spinodal decomposition that accompanies the growth of InGaN can be understood from the material's phase diagram. Thermodynamic calculations by Ho and Stringfellow[4-5] have shown a solid phase miscibility gap between GaN and InN at the temperature normally used during OMVPE growth. This is shown by the material's phase diagram in Figure 3. The area lying inside of the binodal curve defines the alloys and

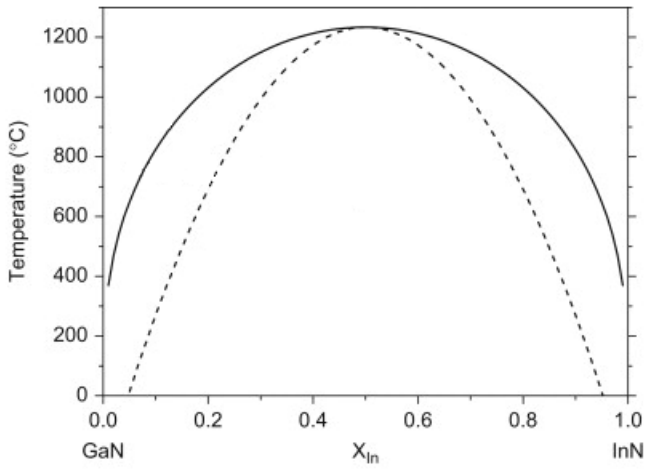

Figure 3 Calculated phase diagram for InGaN from Stringfellow[4] showing binodal (solid) and spinodal (dashed) curves.

temperatures that are thermodynamically unstable. Inside of the binodal curve lies the spinodal curve. Alloys within this region are unstable and are subject to spontaneous phase separation without an energy barrier (spinodal decomposition). Alloys that lie between the binodal and spinodal curves are metastable; hence, an energy barrier must be overcome for phase separation to occur. Outside of the binodal curves, there is complete solid phase miscibility. Alloys in this region are thermodynamically stable and are considered homogeneous. This calculated phase diagram suggests that most useful InGaN alloys require non-equilibrium growth conditions, usually OMVPE or molecular beam epitaxy (MBE), because typical growth

temperatures around 750°C only allow ~5% indium incorporation (others have predicted as low as 2%[6]) into the bulk while typical blue and green LEDs require 15-20% InN concentration. Since there is no thermodynamic barrier to phase separation by spinodal decomposition, it is governed solely by diffusion. During epitaxial growth, surface diffusion is very fast compared to bulk diffusion. This allows phase separation by spinodal decomposition to occur, creating compositional fluctuations within monolayers. Ponce et al. confirmed this experimentally.[7] InGaN with growth conditions lying inside the spinodes had inhomogeneous polycrystalline layers. Other samples with growth conditions lying between the binodal and spinodal curves (metastable region) had secondary phases only at threading dislocations. These dislocations provided sites where phase separation could occur with a reduced energy barrier due to strain relaxation. No spontaneous phase separation in the bulk occurred in these samples. Samples with growth conditions outside the binodal curve were homogeneous, random alloys.

This, however, implies that In-rich and Ga-rich regions would also form within the bulk alloy, but in reality, this effect is almost completely suppressed due to the effect of strain. Formation of In-rich clusters that have a larger equilibrium lattice parameter would have a large free energy penalty so their formation in the bulk is suppressed. On the other hand, defect sites in the material can provide the stain relaxation needed for phase separation. In rich clusters have been experimentally observed at these sites, mostly v-defects.[2,3] Kumar et al. reported a high density of v-defects with In-rich clusters in them when $In_xGaN_{(1-x)}$/GaN (x=0.25 to 0.3) quantum layers were grown by OMVPE.[3] At growth temperatures of 740°C for the GaN barrier layer, they reported seeing the defects and inclusions, while at temperature of 910°C the In-rich clusters were not observed. This could be explained simply by In evaporation at the higher temperature, but another possible mechanism is phase separation driven by spinodal decomposition. The point T=740°C and X_{In}=.25 to.3 falls within the spinodal curve so phase

separation would be favored. On the other hand, the point T=910°C and X_{In} = .25-.3 falls in the metastable region between the binodal and spinodal curves where phase separation would be less favorable due to an energy barrier. Even though phase separation in InGaN has presented growth challenges, it creates a unique microstructure that is involved in the photo emission mechanisms of InGaN.

Emission Mechanisms of InGaN

There has been some debate in the literature regarding this topic. Two different mechanisms have been reported. The first emission mechanism is based on the microstructure of InGaN. The phase separation and inhomogeneity in the material act as quantum wells that localize excitons and enhance the radiative recombination rate. This occurs in compositional fluctuations within epitaxial layers. Although strain suppresses the formation of In-rich clusters in the bulk, this phenomenon has been observed in self organizing quantum dots (QDs) on the surface of the film where more In can incorporate at strain relaxed sites.

The second emission mechanism is also related to the microstructure of the material. The quantum confined Stark effect (QCSE) recombination mechanism is attributed to piezoelectric fields that are present in quantum wells or quantum dots. The fields are the result of strain caused by lattice mismatch between GaN and InGaN. In wurtzitic InGaN, fields are also caused by the inherent piezoelectric properties. These internal electric fields separate the charge carriers in the wells and increase the carrier lifetimes making nonradiative recombination more frequent. The electric field also constrains the allowed energy states within the wells, causing a Stokes shift from the normal emission peaks.[8]

Both of these mechanisms are probably involved in the recombination and emission process. It has been shown that In phase separation effects are likely dominant when In content

in the alloy is relatively high, and piezoelectric effects likely dominate in thicker wells with low In concentration.[9]

Thin Film Growth Modes

Epitaxial growth modes and atomic surface processes are important to understand when analyzing the surfactant effect. Heteroepitaxial growth of semiconductors usually involves strain mechanisms due to a lattice mismatch between substrate and film. Strain affects film growth and morphology and can even produce quantum dots that are utilized in some compound semiconductor devices.[10] Three possible growth modes can occur during epitaxial growth that lead to different surface morphologies. The island growth mode (Figure 4a), otherwise known as Volmer-Weber growth, occurs when adatoms bind more strongly to each other than to the substrate. Hence, atoms preferentially nucleate clusters on the substrate by a 3D growth. Further growth and coarsening of the clusters yields multilayered films with rough surface morphology. In contrast, layer-by-layer growth (Figure 4b), or the Frank-van der Merwe growth mode, occurs when adatoms are more strongly bound to the substrate than to each other. The result is atomically smooth 2D growth in which each monolayer is fully formed prior to growth of the subsequent layers. Layer plus island (Figure 4c), or Stranski-Krastanov growth, is an intermediate case that is characterized by 2D and 3D growth. Initially, a 2D wetting layer, one to a few monolayers thick, is grown on the substrate surface. When a certain critical thickness is reached, a transition from 2D layer-by-layer to 3D island growth occurs. The critical thickness is dependent on the system's free energy and chemical potentials that are determined by chemical and physical properties of the deposit and substrate. Islanding begins when their formation facilitates strain relaxation more efficiently than do flat monolayers. The S-K

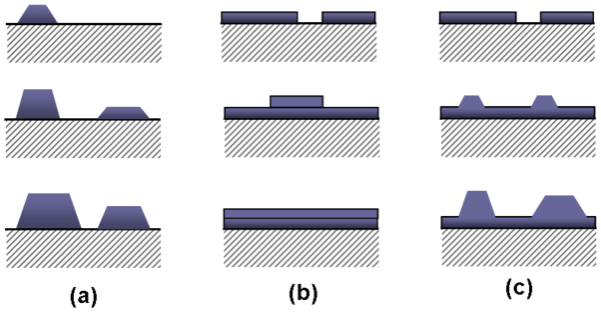

Figure 4 Schematic diagram of the three crystal growth modes: (a) Volmer-Weber growth, (b) Frank-van der Merwe growth, (c) Stranski-Krastanov growth.

mechanism is frequently observed in the heteroepitaxial growth of InGaN yielding self assembled quantum dot structures on the surface.

These growth modes occur by individual atomic processes that are illustrated in Figure 5. During epitaxial growth, individual adatoms diffuse over the surface until they are incorporated into the film by nucleation and binding or step edge attachment, or until they leave the surface by desorption. Interdiffusion can be ignored in most cases because it is very slow relative to the surface processes. These processes are thermally activated and are determined by activation energies and a frequency factor. Surfactants have been used in epitaxial growth to modify surface processes and change activation energies, providing a way to control growth modes.

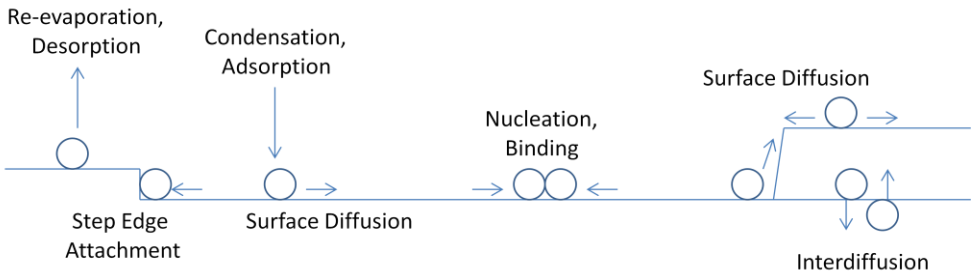

Figure 5 Schematic diagram of the individual atomic surface processes involved in epitaxial growth.

Surfactant Effects

Controlling surface morphology and growth mode during epitaxial growth of thin films is key in producing high quality optoelectronic devices. Surfactants have recently emerged as a powerful tool for controlling epitaxial growth. Surfactants are active surface species that modify surface free energy and have negligible solubility in the bulk, and low desorption coefficients. Sb and Bi are common surfactants used in the growth of InGaN because they are isoelectronic with the bulk so they have no doping effect, and they have comparatively large atomic radii, making incorporation in the bulk very difficult. During the growth process, these elements accumulate on the surface, affecting growth kinetics and, therefore, film morphology. Over the past decade, surfactants have been realized as a valuable tool in controlling epitaxial growth to achieve better devices. Research in surfactant-mediated epitaxial growth has provided a vast

array of varying experimental results but actual surfactant mechanisms have been difficult to understand. Thus far, surfactants have been used to promote either layer-by-layer growth or to increase 3D island growth - both beneficial depending on the device. Most of the experimental work presented in the literature has reported one of these phenomenon depending on the semiconductor material and surfactant used. Experimental results have shown convincing evidence that surfactants can reduce[11,12,13] or increase[11, 14] the adatom surface diffusion length, a key mechanism in the growth process that largely determines the film morphology.

Many of the models presented attempted to explain the surfactant effect in terms of individual atomic processes and thermodynamic aspects at work during epitaxial growth of thin films. Most are based on silicon and germanium systems using heavy group V elements as surfactants (As, Sb, Bi). In this material system, surfactants were attributed to phenomenon like strengthening Ge bonds that lead to nucleation of stress relieving dislocations,[15] creating a (2x1) Sb dimer surface reconstruction,[16] providing an exchange mechanism by which Ge dimers can be embedded under a surfactant layer,[17] providing an exchange mechanism for Si dimers,[18] decreasing the Schwoebel barrier for dimers,[19] and suppressing surface diffusion by providing a low energy barrier Si/As site exchange mechanism.[20] While some of these individual phenomena are likely to occur on the growth surface they do not provide a complete picture or theory of surfactant-mediated growth. The hypotheses do not explain how an individual event, like a dimer exchange, can create a configuration that will nucleate subsequent crystal layers or lead to islands.[21]

A more detailed look at atomistic processes was done by Schroeder et al.[22] In this work, the motion of single Si adatoms on an As surfactant layer was considered by calculating and comparing all the energy barriers for kinetic processes by first-principles energy calculations. The barriers for surface diffusion (0.25 eV) on top of the surfactant layer, and the

adatom/surfactant atom exchange (0.27 eV) and de-exchange (1.1 eV) were compared. They concluded that the de-exchange played an important role in growth process and that while the surfactant layer did provide a decrease in the barrier for surface diffusion, the exchange mechanism acted to suppress surface diffusion because an exchange event would occur quickly. This study, however, still lacked a complete view of the surfactant effect because it lacked an explanation of the nucleation of subsequent layers which would most likely involve many more kinetic barriers that could act as limiting factors.

Other models to explain surfactant-mediated epitaxial growth focused on the effects of strain and surface morphology rather than individual atomic processes. A few of these models took a thermodynamic approach, claiming that surfactant-mediated 3D island suppression was due to the fact that the surfactant layer caused the equilibrium film morphology to be flat and smooth.[21, 23] Eaglesham et al.[24] supported this approach with their experimental analysis of Ge islands in Si. They saw that an Sb surfactant increased the growth rate of Ge (100) island facets on a Si (100) substrate. They concluded that if a surfactant favored facets with the same orientation as the substrate, then 3D island coalescence would occur faster, yielding more layer-by-layer growth. This approach was, however, accompanied with a kinetic argument that surfactants also decreased the diffusion length.

More evidence indicates that the effect of surfactants on heteroepitaxial growth is a kinetic effect, meaning that the equilibrium state of the system is a 3D island morphology and that surfactants slow the approach to equilibrium, suppressing one or more atomic surface processes. One explanation of the surfactant mechanism under the kinetic assumption is that the surfactant atoms suppress surface diffusion. The energy barrier for an adatom to exchange places with a surfactant atom on the growth front and become part of the bulk is much lower than the energy barrier for adatom diffusion. Therefore, an adatom diffuses a very short

distance before attaching to the surface and the saturation density of 2D nuclei rises sharply. Film coalescence occurs quickly and suppresses 3D island formation. Tersoff et al.[25] showed that there is a critical 2D island radius at which a new island will nucleate on top of the existing one. If this radius is small compared to the island spacing, 3D growth will occur. If the radius is large compared to the island spacing, layer-by-layer growth will occur. Surfactant suppressed diffusion and high nucleation density increases 2D island radius and decreases island spacing. Many of the arguments found in the literature are based on this work.

In contrast to these mechanisms, a different approach stems from the correlation of 3D island spacing to diffusion length. It is intuitively obvious that the size and spacing of surface features (islands) are indicative of the surface diffusion length. Consider the case of infinite surface diffusion length. Crystal growth would proceed with layer-by-layer growth because all of the adatoms could reach a step edge or kink and no new islands would nucleate. On the other hand, if adatom diffusion were nonexistent, the growth surface would statistically roughen as more material was deposited.[26] This is, perhaps, a better argument because the exchange mechanism assumes a coherent monolayer of surfactant atoms, which in most cases would be improbable because of misfit strain due to their large size. The same property that keeps surfactant atoms from being incorporated into the bulk would hinder the formation of coherent monolayer coverage. This is also a convincing argument and almost all the explanations found in the literature are based on surfactants changing the surface diffusion length. It is indeed tempting to conclude that the surfactant effect only consists of kinetically limiting or enhancing surface diffusion, as much of the literature suggests, but this is not the entire picture.

In all of these explanations, one essential processe that is key to understanding epitaxial growth is overlooked, step edge attachment. The sticking coefficient, *k*, describes the

probability of incorporation of an adatom that has reached a step edge. Intuitively, adatoms do preferentially incorporate at step edges because they can reach a lower energy state by satisfying more chemical bonds. However, this does not imply that all atoms that reach a step edge are incorporated with 100% probability. The first treatment of this topic was undertaken by Schwoebel et al.[27] They assumed that incorporation of adatoms to kinks or steps was asymmetric, being easier at ascending steps and harder at descending ones. Atoms reaching an ascending step can easily incorporate by striking it, while atoms reaching a descending step have to overcome an additional energy barrier, termed the Schwoebel barrier, before incorporation into the layer. This must be taken into account when creating an accurate model for the surfactant effect. Neglecting step edge incorporation and the Schwoebel barrier in a treatment of the surfactant effect leads to incorrect conclusions about the surface diffusion length. All previous explanations identifying surface diffusion as the only relevant process inadvertently assume that the sticking coefficient is unity and, therefore, incorrect conclusions result. For example, assuming k=1, a higher island density could indeed indicate a shorter surface diffusion length because of the smaller island spacing. But, a higher island density could also be the result of a decrease in the value of k. If, say, k=0.1, less step edge attachment and more island nucleation would occur even if the surface diffusion length has increased.

Another interesting model was presented that tried to account for the change in sticking coefficient. Many previous models were supported by experimental evidence particularly by Voigtlander et al.[28] They studied the effects of submonolayer epitaxial growth in Si and Si/Ge systems in the presence of a surfactant. They concluded that there were two general types of surfactants, group III and IV elements which promoted 3D island growth and group V and VI elements which promoted layer-by-layer growth. The idea for a new model arose from the fact that surfactants preferring lower coordination should in fact, passivate the Si/Ge surface more

effectively than do surfactants that prefer higher coordination, i.e., group V and VI materials should be more effective than group III and IV materials. A more highly passivated surface should provide faster surface diffusion for adatoms while less passivation should suppress diffusion. Experimental results of Voigtlander et al., however, showed the opposite. To reconcile the experimental results with theory, Kandel and Efthimios[21] proposed the diffusion-de-exchange-passivation (DDP) model. This model took into account not only surface diffusion but also step edge processes. The processes they considered are shown in Figure 6. These are shown as (a) the diffusion of adatoms on top of a monolayer of surfactant molecules, (b) the exchange of adatoms with surfactant atoms on a terrace or a step, (c) de-exchange of adatoms with surfactant atoms, and lastly, exchange (d) and de-exchange (e) when surfactants cannot passivate step edges. Activation energies were calculated for all of these events and Monte Carlo simulations were carried out to determine what role each of these processes played in surfactant-mediated growth. The events in the simulation occurred randomly at rates that were defined by their activation energies. They concluded, as others have observed, that there were two possible outcomes of the surfactant effect which depend on the combination of materials and surfactant, an increase in layer-by-layer growth or 3D islanding. They also concluded that this effect was not due to a change in surface diffusion, but a passivation effect of the surfactant step edges.

This effect can be explained in term of the details of S-K growth. The onset of 3D islands occurs when they facilitate more efficient strain relaxation than flat layers do. The size of the island is kinetically limited by detachment of adatoms from step edges due to strain.[29] A monolayer coverage of surfactant that is capable of passivating step edges would also suppress

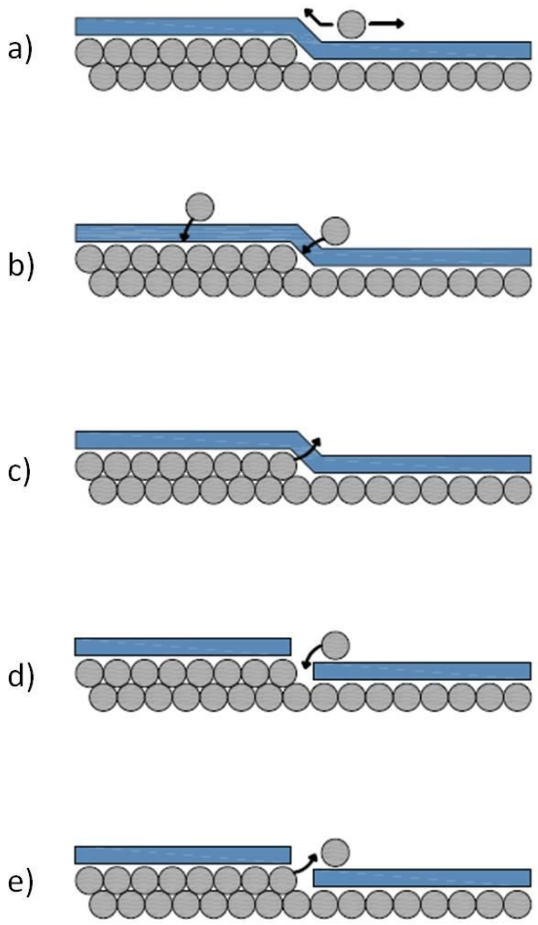

Figure 6 Schematic diagram of the surface processes involved in the DDP surfactant effect model of Kandel and Efthimios[21] : (a) the diffusion of adatoms on top of the surfactant molecules, (b) the exchange of adatoms with surfactant atoms on a terrace or a step, (c) de-exchange of adatoms with surfactant atoms, (d) exchange when surfactants cannot passivate step edges, (e) de-exchange when surfactants cannot passivate step edges.

detachment events.[21] This mechanism would allow a surfactant to change the growth mode from 3D to later-by-layer even if surface diffusion was not affected. On the other hand, if a surfactant could not passivate a step edge, 3D growth would be enhanced regardless of the effect on surface diffusion. The ability of a surfactant to passivate a step edge would vary widely depending on its valence, preferred coordination, and size, and does not necessarily coincide with its ability to passivate a flat surface.

The DDP model takes into account more of the atomic processes one must consider when analyzing the surfactant effect but it is still rather far from being a comprehensive model of surfactant-mediated epitaxial growth. Such a simple model fails to take into account many aspects of a real scenario that may be very important to the whole process. The model is also based on idealized assumptions that could deviate somewhat from reality. Diffusion and exchange pathways were postulated based on possible surface reconstruction, an crucial aspect that could entirely change the results of the experiment. It also assumes that the diffusion, exchange, and de-exchange of only one atomic species controls the process, and that perfect monolayer surfactant coverage exists. In addition, most models, including this one, are derived from experimental results based on Si/Si or Si/Ge systems. It would be rash to assume that no deviations from these models would be needed to accurately explain the surface science of nitride semiconductors. For example, the growth rate of OMVPE grown GaN is dependent on the mass transport of Ga, but some evidence has shown that the growth mode might be somewhat dependent on Ga and N surface diffusion. A model assuming that only the actions of one species controls the growth process would not be sufficient in this case.

DFT calculations by Gokhale et al.[30] have given many insights into the growth of GaN and the effects of surfactants. These calculations compared the effect of Sb and Bi on GaN. In particular, the calculations compared the adsorption and diffusion of atomic species on the

surface of GaN and also the reaction paths for steps leading to the formation of N_2, SbN, and BiN. The diffusion barriers for SbN and BiN intermediates on the GaN surface were then compared in order to study the surfactant effect on the growth process.

The calculations showed that N diffusion was the rate limiting step in the overall GaN growth process. Accordingly, increasing the mobility of N on the surface would noticeably affect properties such as surface roughness. On the GaN (0001) surface, the energy barrier for the recombination of N atoms to form N_2 is much higher than the energy barrier for the formation of SbN or BiN, meaning that these intermediates could form abundantly on the surface. Furthermore, the calculated surface diffusion barrier for atomic N (0.99eV) is higher than the barrier for SbN (0.69eV) and BiN (0.90eV). The lower energy barriers for these intermediate compounds would greatly increase their diffusion and therefore, increase N transport on the surface, allowing more uniform, smooth, layer by layer growth. If Arrhenius dependence for the diffusion coefficient is assumed, and standard OMVPE growth temperatures for GaN are also assumed, the diffusion coefficient for SbN is roughly 14 times larger than that of atomic N, and the diffusion length is increased almost four-fold. Although the BiN diffusion barrier is higher than that of SbN, it still leads to a significant increase in the diffusion length – around 50%.

For the group III nitride semiconductors, GaN in particular, studies have shown evidence that nitrogen incorporation is more favorable at step sites during epitaxial growth[31]. This is most likely due to the higher number of dangling bonds at those sites, facilitating more dissociation reactions and N incorporation. One would, therefore, expect the Sb and Bi to allow more nitrogen to diffuse to these sites giving higher N incorporation. This would affect the growth quality of GaN due to the fact that N diffusion was calculated to be the rate limiting step. Layers would be able to grow more uniformly with less average surface roughness. This conclusion is supported by a few experiments in OMVPE growth of GaN using Sb as surfactant.[32-

[33] When SbN or BiN reached a step edge, the dangling bonds would aid the decomposition of the intermediate N compounds, liberating Sb or Bi. Due to their relative size, higher vapor pressure (relative to Ga), and weaker bonding with the epitaxial layer, Sb and Bi are not consumed or incorporated (to any significant degree) into the solid by this process and, therefore, perform a catalytic role for surface diffusion of atomic N.

Understanding and determining surface reconstruction is another key factor in determining surfactant effects on epitaxial growth. Surface reconstruction can determine much in terms of growth mode and the resulting surface morphology, i.e., $CuPt_B$ ordering in GaInP. This is caused by P-dimers on the surface that have a comparatively short bond length.[34] They form a periodic array of tensile and compressive strain that provides the driving force for ordering. The smaller group III atom prefers the compressive site and the larger group V atom prefers the tensile site. This creates planes of alternating atomic species in the bulk. When a surfactant is used, a different surface reconstruction occurs that removes the periodic array of tensile and compressive forces and leads to a more random mixture. Other experimental results in the literature have also shown evidence of a change in surface reconstruction brought on by surfactant. Zang et al.[32] showed that during the lateral epitaxial overgrowth (LEO) of GaN with Sb surfactant there was a marked shift in the facet formation. LEO growth without surfactant resulted in sloped $\{1\bar{1}01\}$ facets that gave a triangular cross section while growth with 1.5% Sb surfactant resulted in vertical $\{11\bar{2}0\}$ facets and a rectangular cross section. Samples grown with higher levels of Sb showed the same results only with higher growth rates. The authors hypothesized that the surfactant effect was a kinetic one, that of Sb enhancing the desorption or impeding the surface decomposition of NH_3. This effect would be analogous to a lower V/III input ratio during the growth process leading to enhanced Ga diffusion on the surface. Another consideration is that a change in surface reconstruction caused by Sb could also create the

dramatic change in growth facets from the 0% to the 1.5% samples. Assuming that Sb effectively enhanced only the diffusion of Ga on the surface, one could expect the changes in morphology to be somewhat linear with increasing surfactant. But if a change in surface reconstruction occurred at a certain concentration of Sb, one could expect a monotonic change in the surface morphology, as is seen with the drastic change in facet formation. A new surface reconstruction would redefine all the energy barriers for surface processes on different facets and cause a shift in the growth mode. A similar phenomenon involving a surface phase change was observed by Ok et al.[33] during hydride vapor phase epitaxy of InGaN with Sb. They reported a change in the orientation of InGaN nanostructures (QDs) when Sb was present during growth. Without Sb they observed hexagonal nanostructures aligned vertically to the $\{0001\}$ substrate. The presence of Sb induced parallel alignment of the QDs with the substrate, along with a lower surface coverage density.

These explanations of surfactant-mediated growth are far from comprehensive models, and it is apparently unlikely that a single model could explain all surfactant effects, but the basic phenomena presented in them outline our current understanding of the processes involved. These include surfactant modified surface diffusion, sticking coefficient, and surface reconstruction. The objective of our experiments is to provide further insight to the surfactant effect of Sb on OMVPE grown InGaN films.

EXPERIMENTAL PROCEDURES

InGaN was grown on 2 inch (0001) sapphire wafers by OMVPE at 720°C. The TMIn/(TMIn+TMGa) ratio was 0.64, and the growth rate was 0.39Å/s. A GaN buffer layer was deposited on the sapphire prior to epitaxial growth of InGaN. In order to test the effects of TMSb on the growth process and resulting film characteristics, different samples were grown with varying values of TMSb/(TMIn+TMGa) in the vapor. The first test batch consisted of samples grown with 0%, 0.5%, 1%, and 2% TMSb. These samples were grown with two different approximate average film thicknesses, 1.5 nm (38 second growth time) and 3 nm (75 second growth time). Another batch was grown with TMSb concentrations of 0.75%, 1.25%, 1.75%, and 2.5% with a average film thickness of 3 nm. All other growth parameters were unchanged.

Characterization of the samples was conducted to determine surface morphology, In incorporation, and photo emission spectra. PL was performed with a 349 nm high intensity laser. AFM was done with a Brunker Dimension Icon apparatus operating in the quantum nano-mechanical mapping mode.

RESULTS

Photoluminescence spectra from each sample showed a large characteristic GaN peak from the underlying buffer layer, and a smaller peak caused by the InGaN film. Figure 7 shows the spectra for each sample from 425-625nm so that the Sb-induced peak shift can be seen. A marked shift in the emission peak from blue to green is seen between the 1% and 1.25% sample. There was a sharp decline in the intensity of the InGaN peak compared to the GaN as the Sb concentration increased (characteristic of the "green gap"), but no attempt was made to compare the peak intensity or luminescent efficiency. The spectra also showed interference pattern oscillations which were an important indication that these emissions originated at the top in the InGaN thin film, and were not due to the yellow emission of GaN, which would be produced within the GaN in a spatially distributed manner so would not give an interference pattern. The oscillations were not observed in the large characteristic GaN peak.

The bandgap of each sample was taken from its respective PL peak. The bandgap of $In_xGa_{1-x}N$ depends on the value of *x* and ranges from that of InN (0.7eV) to that of GaN (3.4eV). Equation 1 gives the bandgap energy as a function of alloy composition and In incorporation was calculated from this relationship.[35] Figure 8 shows the bandgap and In incorporation in the film as a function of Sb concentration. An abrupt change in the bandgap energy and alloy composition was observed in samples with greater than 1% Sb. The bandgap was shifted from 2.3 eV to 2.7 eV corresponding to a shift in In concentration from 18% to 31%. The photoluminescence spectra were confirmed by NSOM data but the spatial resolution of this technique was not high enough to give any additional data.

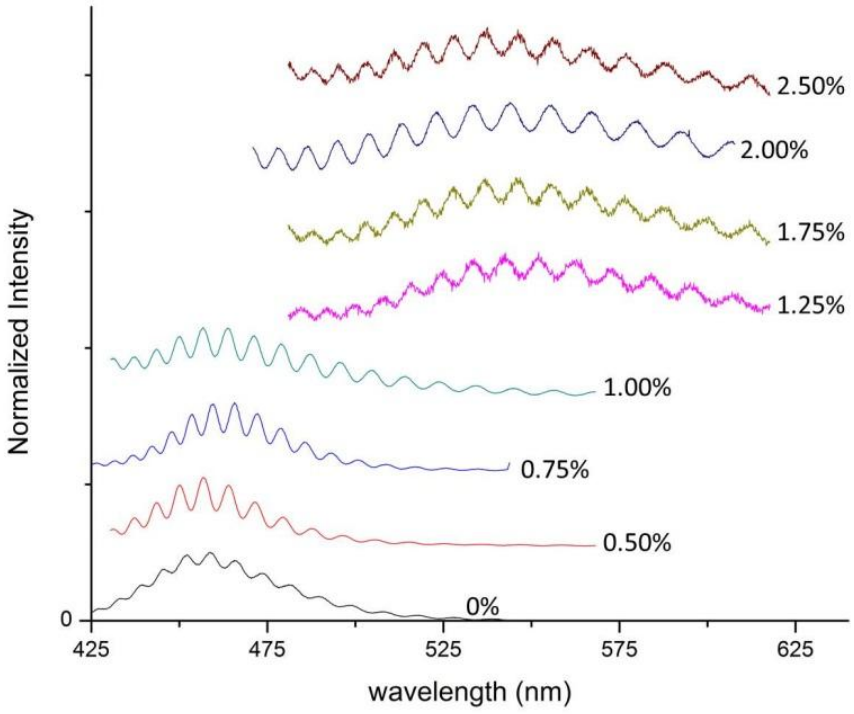

Figure 7 Normalized PL emission spectra comparison shown from 425-625 nm illustrating the In peak shift due to addition of Sb to the growth process

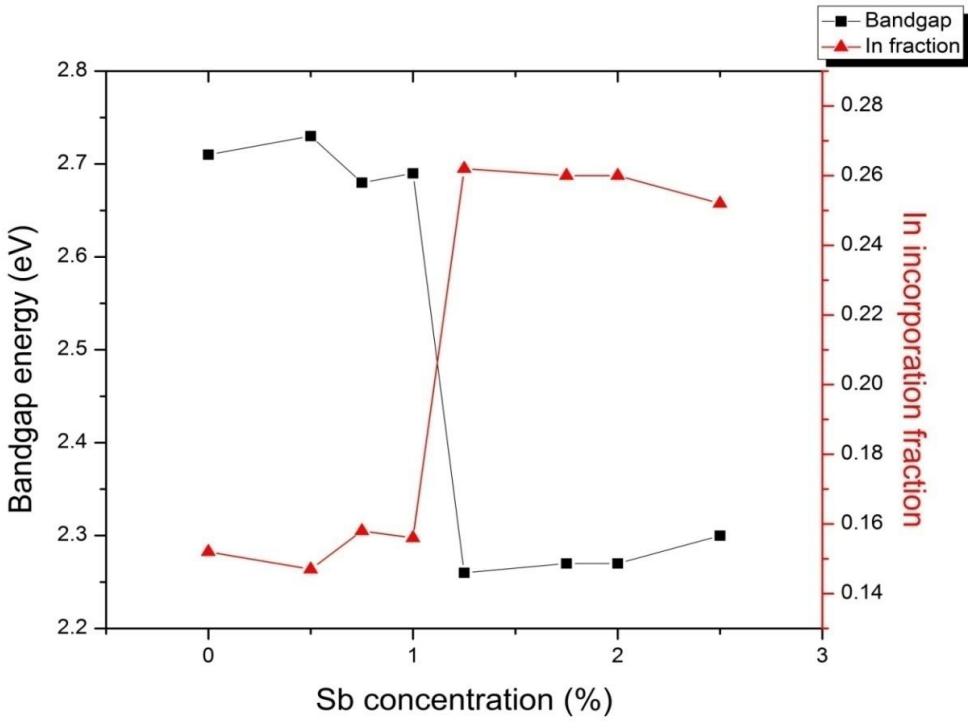

Figure 8 Bandgap energy and In incorporation versus Sb concentration, calculated using Equation 1 and the PL emission peak values from Figure 9.

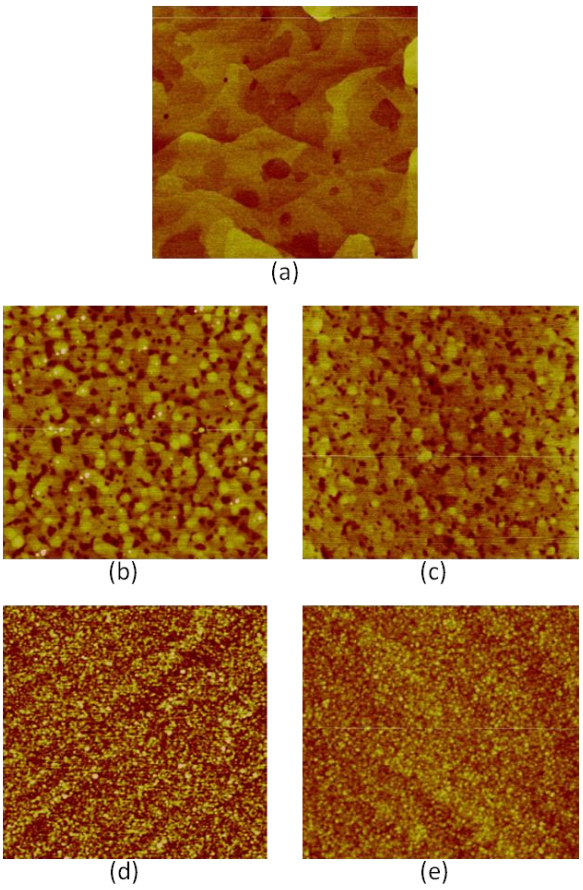

Figure 9 1x1 µm AFM images of OMVPE grown InGaN with varying amounts of Sb surfactant, representing the three different morphologies observed. Images (a)-(e) show InGaN grown with 0%, 0.5%, 1%, 1.25%, and 2% Sb respectively.

AFM images (1x1µm) showed the Sb-induced changes in surface morphology. Figure 9(a) shows the surface of InGaN produced under normal conditions with no surfactant present during growth. Figure 9(b) and 9(c) show the change in morphology with the addition of up to 1% Sb to the growth process. Island density increased, island size decreased, and the surface roughened. Another change in morphology occurred at Sb concentrations above 1%, with a dramatic increase in island density, size, and shape, as seen in Figure 9(d) and 9(e).

$$E_g = 3.42eV - x2.65eV - x(1-x)2.4eV \quad (1)$$

Figure 10 shows AFM line scan height profile comparisons for some of the samples. The line scans seemed to show holes or pits on the surface. The maximum depth of the holes was 2nm on the 0.5% and 1% sample and 1nm on the 2% sample. The difference was most likely due the larger islands on the 0.5% and 1% samples not having coalesced like the islands on the 2% sample, which had a much higher island density. The 0% sample showed islands and valleys but did not have the same characteristic holes that the other rougher samples had. The film quality was very good as no v-defects or nanopipes were observed by either AFM or STEM. SEM images showed similar trends but most of the discernible features were pits on the surface where film coalescence had not yet occurred. These were not characteristic of v-pits or v-defects as they did not propagate through the film.

STEM was performed on cross sections of the 1% and 2% samples. The cross sectional image of the 1% sample is shown in Figure 11. This shows the GaN buffer layer, InGaN film, and the islands or quantum dots (QDs) on the film surface. Comparison of the 1% and 2% samples seen in Figure 12 also showed a marked change in the film morphology with a qualitative difference in the size and shape of the quantum dots on the surface. The 2% sample showed smaller, more densely packed QDs than the 1% sample, consistent with the AFM images. Concentration profiles of In and Ga were taken on the film cross sections (Figure 12). The 1% sample showed a spike in indium concentration across the InGaN thin film between the GaN and QD layer. In contrast, the 2% sample showed a spike in indium concentration in the QD layer.

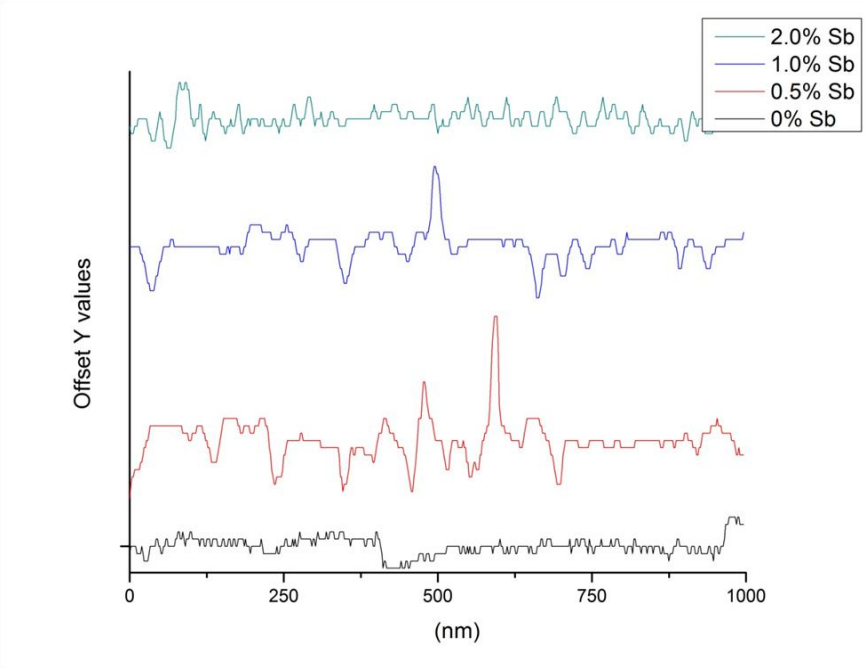

Figure 10 AFM line scans showing height profiles of the surfaces. The 0% sample is very smooth. The 0.5% and 1% samples show a rough surface phase with large 3D islanding. The 2% sample shows a different surface phase with smaller, densely packed 3D islands (characteristic of the 1.25%-2.5% samples).

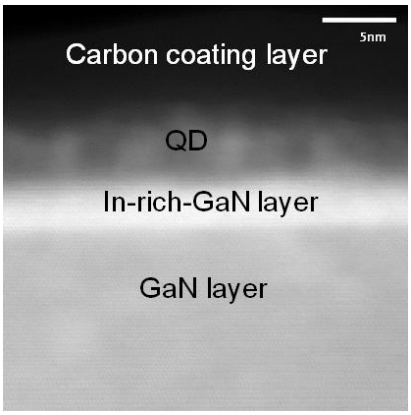

Figure 11 Cross sectional STEM image of the sample grown with 1% Sb, showing the underlying GaN layer, the InGaN thin film layer, the QDs on top of the film. The Carbon coating layer was added for STEM imaging.

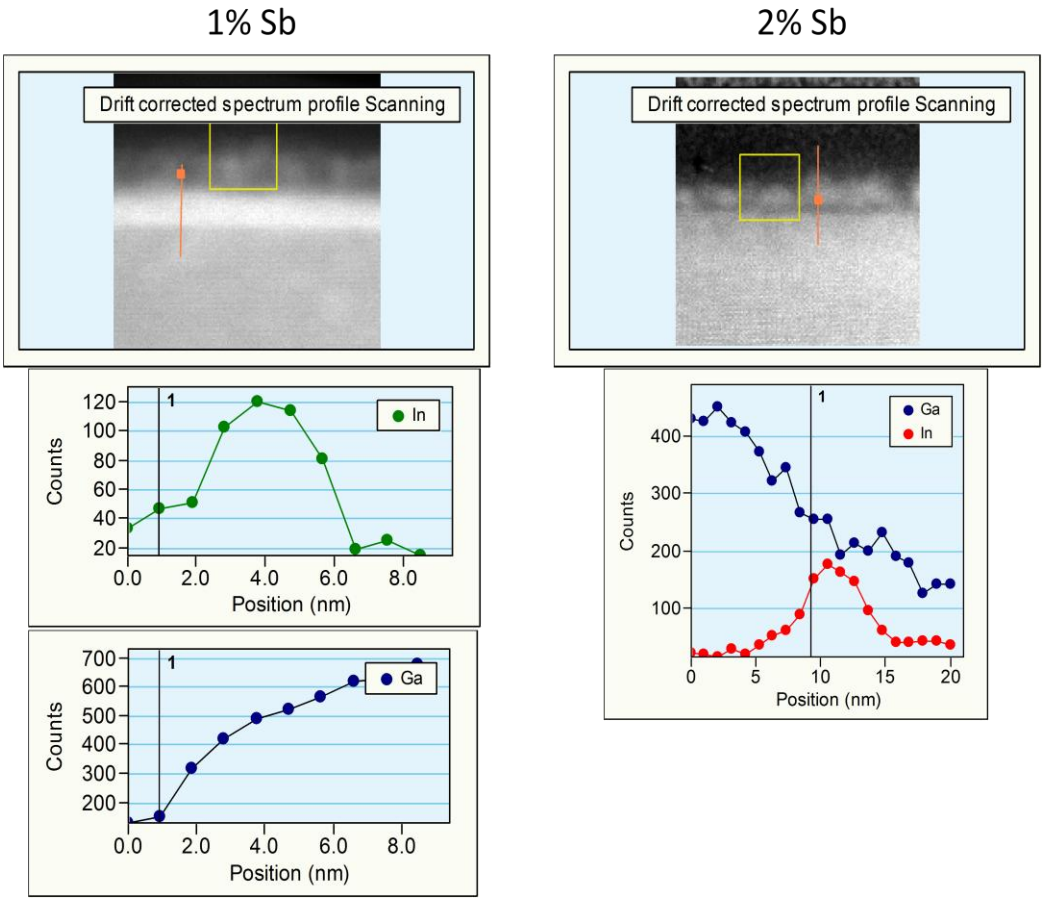

Figure 12 STEM data showing In and Ga concentration profiles in the film. Note that the line scan direction is down for the 1% sample and up for the 2% sample.

DISCUSSION

The magnitude of the surfactant effect was dependent on Sb concentration. The initial effect, when 0.5% Sb is added to the growth process, was a shift to 3D island formation. The island density only increased very slightly with Sb from 0.5% to 1%. This effect was only seen in the AFM results because the PL emission peaks for these samples were the same, indicating that the In concentration and distribution was relatively the same from sample to sample. If a reasonable assumption was made that strain inhibits Sb from forming a coherent monolayer on the surface because of its size, then the exchange/de-exchange surfactant effect mechanism would not be valid and another mechanism must be considered. The change in surface morphology could be due to a surfactant-induced decrease in the surface diffusion length or a decrease in sticking coefficient. If we assumed that, due to strain and high surface mobility, the large Sb atoms would accumulate at step edges, then we would also expect the surface diffusion length to increase because Sb was occupying adsorption sites. This is clearly not the case because this would lead to smoother layer-by-layer growth. However, if the sticking coefficient was decreased by Sb occupying step edges, more 3D island nucleation would occur. This is a more likely explanation because it could explain some of the observed results. This explanation could well be an oversimplification but is nonetheless useful in analyzing the surfactant effect. In reality, the surface diffusion length and sticking coefficient are somewhat dependent on each other and complications arise when trying to separate their effects.

Another effect occurs at Sb concentrations above 1%. At this critical concentration, there is a drastic change in island size, shape, and density seen by AFM. The PL emission peak is

also shifted to a longer wavelength indicating a higher In concentration or a different emission mechanism. If this surfactant induced change was solely based on the aforementioned mechanism, i.e., surfactant induced changes in surface diffusion and sticking coefficient, a more gradual change in surface morphology and emission peak would be expected.

The abrupt change in In incorporation observed here is suggestive of a phase change, in this case, a phase change of the surface reconstruction induced by the addition of Sb to the surface. Wixom et al. [34, 36] calculated the surface phase diagram for GaP and InP as a function of Sb, showing a number of different surface reconstructions depending on the Sb concentration in the vapor phase. Of course, the surface reconstructions involving Sb on GaN are unknown. Studies on GaInP have clearly shown that the structure (i.e., reconstruction) of the growth surface can have profound effects on the microstructure, in this case, the atomic scale ordering of the material.[36-37] Different surface reconstructions provide the thermodynamic driving force for different microstructures and hence, markedly different bandgap energies. Surface reconstruction has also changed the morphology of GaAs grown by OMVPE by changing surface diffusion and attachment at step edges.[26, 38]

Assuming that the InGaN surface reconstruction is dependent on the Sb concentration, the abrupt changes in In incorporation seen in Figure 8 could be due to a surface phase change at the critical Sb concentration. In contrast to this explanation of the results, changes in surface kinetics due to Sb on the surface would presumably give smoothly varying dependence of In incorporation on $(Sb/III)_v$, as opposed to the abrupt change observed. The abrupt change in bandgap and solid composition was also reflected in the surface morphology of the films seen by AFM, and coincided with the idea of a surface phase change due to surfactant coverage because of the different morphologies seen above and below the critical Sb concentration.

Island density increased and island size decreased with the addition of Sb to the growth process. Samples grown with Sb concentrations from 0.5% to 1%, showed a distinct morphology that did not change substantially with increasing Sb. Island size and density remained relatively constant in this regime. Samples grown with Sb concentrations from 1.25% to 2.5% showed another distinct morphology with no substantial change in island size or density with increasing Sb. The abrupt change observed in surface morphology and PL emission spectra at a particular Sb surface coverage is difficult to explain only in terms of surfactant modified atomic surface processes such as diffusion and step-edge attachment, as is often done in the literature, but more likely indicates a surfactant-induced change in surface reconstruction. Other surfactant studies on the nitrides showed similar phenomenon that could be explained in terms of a surface phase change. The abrupt change in the growth facets of LEO GaN with the addition of Sb (Zhang et al.[32]) could be attributed to a change in surface reconstruction. The authors attributed this to Sb affecting the fundamental surface processes during growth, such as adsorption/desorption, diffusion, and surface decomposition of precursors. However, given the sudden, striking change in the shape of these LEO GaN stripes, in light of the observations reported here, these results could also be interpreted as a surfactant-induced surface phase change leading to new film morphology.

Other evidence that could be interpreted as a surfactant-induced phase change was seen in HVPE grown InGaN with Sb. Ok et al.[33] reported a surfactant-induced shift in the orientation of hexagonal InGaN nanostructures. Without Sb, these structures were vertically aligned with the growth plane. With the addition of Sb, they grew parallel to the growth plane. The apparent density of nanostructures on the surface also appeared to be much lower when grown in the presence of Sb (from Figure 4 of Ok et al.). The PL emission spectra of their samples showed a striking similarity to our data. The emission peak of the surfactant-enhanced

sample was shifted to a much lower energy, indicating a higher In incorporation in the film, consistent with our samples that were grown above the critical Sb concentration. The abrupt change in surface morphology, PL peak energy, and the associated solid composition, could be interpreted as a surface phase change just as these results have been interpreted.

STEM data indicated a redistribution of the In to the islands or QDs on the surface rather than the underlying thin film layer. This could be a result of a different surface reconstruction. Niu et al.[39] showed that In atoms prefer to redistribute on the top surfaces of QDs due to strain relaxation. This explanation could also account for a shift in emission peak because island surfaces with high In content could act as quantum wells for radiative recombination of charge carriers. Different Sb induced surface reconstruction would provide different thermodynamic driving forces that could favor higher In content. One possible mechanism is a surface reconstruction that provides fasters diffusion, allowing for more phase separation of InN into quantum dot like structures and less In surface desorption.

The InGaN PL peak intensity decreased drastically with increased Sb. This phenomenon has also been observed by others in high In content InGaN. It has been hypothesized that this is due to increased In incorporation producing more strain induced defects in the material that decrease optical efficiency by providing non-radiative recombination sites.[1] It could also be due to the quantum-confined Stark effect that occurs in high In content InGaN. In this case, an internal electric field causes the physical separation of charge carriers, making recombination less efficient. Both of these theories have been presented as possible reasons for the decrease in peak intensity, but no direct evidence of either was observed in these samples.

Some disagreement has occurred in the literature on whether the surfactant effect in heteroepitaxy is a thermodynamic or kinetic effect[21]. This debate is centered on the surfactant induced suppression of 3D islands. Although this experiment deals with surfactant-induced

islands, it suggests that it is a thermodynamic effect by showing evidence of a surfactant induced change in surface reconstruction. A new surface reconstruction in the presence of surfactant would create a thermodynamic driving force for different surface and bulk phases.

CONCLUSION

In summary, a review of InGaN materials and surfactant effect in heteroepitaxial growth has been presented. The use of surfactants can change the growth mode by altering the kinetics and thermodynamic driving forces of surface processes and surface reconstruction. Surfactants have been seen to either promote layer-by-layer growth or 3D island growth by altering the surface diffusion length and sticking coefficient. In other cases, they have been seen to alter surface reconstruction, providing or removing the driving force for ordering in semiconductor alloys. These fundamentals have been applied to understanding the effect of Sb on InGaN. Different samples of InGaN grown with varying amounts of Sb (0%-2.5%) were characterized by AFM, PL, NSOM, SEM, and STEM. Sb was observed to enhance 3D island formation in InGaN. These methods revealed an abrupt change in bandgap, solid composition, and surface morphology of films at a certain critical surfactant concentration. Above and below this threshold concentration of approximately 1% Sb, two distinct regimes of surface morphology and PL emission characteristics were observed. This marked change in morphology and emission was interpreted as due to a surfactant induced change of surface phase on the InGaN films, similar to what has previously been observed in GaInP. A new surface phase could provide the driving force for a different In incorporation or distribution on the growth front. If the surfactant effect was only to changes surface diffusion or sticking coefficient, a more gradual change would be expected and the bimodal form of Figure 8 (bandgap energy and In incorporation as a function of Sb concentration) would not be observed. This conclusion is

supported by STEM data that shows different In distribution between the samples grown with 1% and 2% Sb.

Further experimental work is needed to confirm these conclusions. *In situ* surface photoabsorption (SPA) measurement during OMVPE growth would be needed to confirm and identify different surface reconstructions. The remaining samples also need to be characterized by STEM in order to confirm the difference in In distribution. First principles calculations could also aid in determining the surfactant mechanism by analyzing different surface reconstructions.

InGaN is an important semiconductor alloy that will further be utilized in optoelectronic devices. Surfactants will continue to be a vital tool in controlling the epitaxial growth and microstructure of this material. This experiment has demonstrated a new surfactant effect of Sb on InGaN that will be important in materials processing for optoelectronic devices.

REFERENCES

1. Yam, F. K.; Hassan, Z., InGaN: An overview of the growth kinetics, physical properties and emission mechanisms. *Superlattices and Microstructures* **2008,** *43* (1), 1-23.

2. Suihkonen, S.; Lang, T.; Svensk, O.; Sormunen, J.; Törmä, P. T.; Sopanen, M.; Lipsanen, H.; Odnoblyudov, M. A.; Bougrov, V. E., Control of the morphology of InGaN/GaN quantum wells grown by metalorganic chemical vapor deposition. *Journal of Crystal Growth* **2007,** *300* (2), 324-329.

3. Kumar, M. S.; Lee, Y. S.; Park, J. Y.; Chung, S. J.; Hong, C. H.; Suh, E. K., Surface morphological studies of green InGaN/GaN multi-quantum wells grown by using MOCVD. *Materials Chemistry and Physics* **2009,** *113* (1), 192-195.

4. Stringfellow, G. B., Microstructures produced during the epitaxial growth of InGaN alloys. *Journal of Crystal Growth* **2010,** *312* (6), 735-749.

5. Ho, I.-h.; Stringfellow, G. B., Solid phase immiscibility in GaInN. *Applied Physics Letters* **1996,** *69* (18), 2701-2703.

6. Gan, C. K.; Feng, Y. P.; Srolovitz, D. J., First-principles calculation of the thermodynamics of In_{x}Ga_{1−x}N alloys: Effect of lattice vibrations. *Physical Review B* **2006,** *73* (23), 235214.

7. Ponce, F. A.; Srinivasan, S.; Bell, A.; Geng, L.; Liu, R.; Stevens, M.; Cai, J.; Omiya, H.; Marui, H.; Tanaka, S., Microstructure and electronic properties of InGaN alloys. *physica status solidi (b)* **2003,** *240* (2), 273-284.

8. Damilano, B.; Grandjean, N.; Massies, J.; Siozade, L.; Leymarie, J., InGaN/GaN quantum wells grown by molecular-beam epitaxy emitting from blue to red at 300 K. *Applied Physics Letters* **2000,** *77* (9), 1268-1270.

9. Shapiro N.A., P. P., Kieielowski C., Mattos L.S., Yang J.W., Weber E.R., MRS Internet J. Nitride Semicond. Res. **2000,** *5*, 1.

10. Liu, F.; Lagally, M. G., Self-organized nanoscale structures in SiGe films. *Surface Science* **1997,** *386* (1–3), 169-181.

11. Massies, J.; Grandjean, N., Surfactant effect on the surface diffusion length in epitaxial growth. *Physical Review B* **1993,** *48* (11), 8502-8505.

12. Grandjean, N.; Massies, J.; Etgens, V. H., Delayed relaxation by surfactant action in highly strained III-V semiconductor epitaxial layers. *Physical Review Letters* **1992,** *69* (5), 796-799.

13. Tromp, R. M.; Reuter, M. C., Local dimer exchange in surfactant-mediated epitaxial growth. *Physical Review Letters* **1992,** *68* (7), 954-957.

14. (a) Nakahara, H.; Ichikawa, M., Molecular beam epitaxial growth of Si on Ga-activated Si(111) surface. *Applied Physics Letters* **1992,** *61* (13), 1531-1533; (b) Iwanari, S.; Takayanagi, K., Surfactant epitaxy of Si on Si(111) surface mediated by a Sn layer I. Reflection electron microscope observation of the growth with and without a Sn layer mediate the step flow. *Journal of Crystal Growth* **1992,** *119* (3–4), 229-240.

15. S.J. Nakamura, H. K., T. Osaka, Surfactant-Induced Bond Strengthening in As-Grown Film Surfaces. *Japanese Journal of Applied Physics* **1996,** *35*, L441-L443.

16. Jenkins, S. J.; Srivastava, G. P., Bonding and structure of the Si(001)(2 × 1)-Sb surface. *Surface Science* **1996,** *352–354* (0), 411-415.

17. Yu, B. D.; Oshiyama, A., Diffusion and dimer exchange in surfactant-mediated epitaxial growth. *Physical Review Letters* **1994,** *72* (20), 3190-3193.

18. Ohno, T., Site exchange mechanism in surfactant-mediated epitaxial growth. *Physical Review Letters* **1994,** *73* (3), 460-463.

19. Oh, C. W.; Kim, E.; Lee, Y. H., Kinetic Role of a Surfactant in Island Formation. *Physical Review Letters* **1996,** *76* (5), 776-779.

20. Ko, Y.-J.; Yi, J.-Y.; Park, S.-J.; Lee, E.-H.; Chang, K. J., Single Adatom Exchange in Surfactant-Mediated Epitaxial Growth. *Physical Review Letters* **1996,** *76* (17), 3160-3163.

21. D. Kandel, E. K., The Surfactant Effect in Semiconductor Thin Film Growth. In *Solid State Physics*, H. Ehrenreich, F. S., Ed. Academic Press: San Diego, 2000; Vol. 54.

22. Schroeder, K.; Engels, B.; Richard, P.; Blügel, S., Reexchange Controlled Diffusion in Surfactant-Mediated Epitaxial Growth: Si on As-Terminated Si(111). *Physical Review Letters* **1998,** *80* (13), 2873-2876.

23. Kern, R.; Müller, P., Three-dimensional towards two-dimensional coherent epitaxy initiated by surfactants. *Journal of Crystal Growth* **1995,** *146* (1–4), 193-197.

24. Eaglesham, D. J.; Unterwald, F. C.; Jacobson, D. C., Growth morphology and the equilibrium shape: The role of ‘‘surfactants’’ in Ge/Si island formation. *Physical Review Letters* **1993,** *70* (7), 966-969.

25. Tersoff, J.; Denier van der Gon, A. W.; Tromp, R. M., Critical island size for layer-by-layer growth. *Physical Review Letters* **1994,** *72* (2), 266-269.

26. Wixom, R. R.; Rieth, L. W.; Stringfellow, G. B., Sb and Bi surfactant effects on homo-epitaxy of GaAs on (0 0 1) patterned substrates. *Journal of Crystal Growth* **2004,** *265* (3–4), 367-374.

27. Schwoebel, R. L.; Shipsey, E. J., Step Motion on Crystal Surfaces. *Journal of Applied Physics* **1966,** *37* (10), 3682-3686.

28. Voigtländer, B.; Zinner, A.; Weber, T.; Bonzel, H. P., Modification of growth kinetics in surfactant-mediated epitaxy. *Physical Review B* **1995,** *51* (12), 7583-7591.

29. Tersoff, J.; Tromp, R. M., Shape transition in growth of strained islands: Spontaneous formation of quantum wires. *Physical Review Letters* **1993,** *70* (18), 2782-2785.

30. Gokhale, A. A.; Kuech, T. F.; Mavrikakis, M., A theoretical comparative study of the surfactant effect of Sb and Bi on GaN growth. *Journal of Crystal Growth* **2007,** *303* (2), 493-499.

31. Yuen, H. B.; Bank, S. R.; Bae, H.; Wistey, M. A.; Harris, J. J. S., The role of antimony on properties of widely varying GaInNAsSb compositions. *Journal of Applied Physics* **2006,** *99* (9), 093504-8.

32. Zhang, L.; Tang, H. F.; Kuech, T. F., Effect of Sb as a surfactant during the lateral epitaxial overgrowth of GaN by metalorganic vapor phase epitaxy. *Applied Physics Letters* **2001,** *79* (19), 3059-3061.

33. Ok Jin Eun, J. D. W., Jeon Hun Soo, Lee Ah Reum, Lee Gang Suok, Kim Kyung Hwa, Ahn Hyung Soo, Yang Min, Structural Change of InGaN Nanostructures Grown by Mixed-Source Hydride Vapor Phase Epitaxy. *Japanese Journal of Applied Physics* **2011,** *50* (1).

34. Wixom, R. R.; Modine, N. A.; Stringfellow, G. B., Theory of surfactant (Sb) induced reconstructions on InP(001). *Physical Review B* **2003,** *67* (11), 115309.

35. Wu, J.; Walukiewicz, W.; Yu, K. M.; Ager Iii, J. W.; Haller, E. E.; Lu, H.; Schaff, W. J., Narrow bandgap group III-nitride alloys. *physica status solidi (b)* **2003,** *240* (2), 412-416.

36. Wixom, R. R.; Stringfellow, G. B.; Modine, N. A., Theory of Sb-induced triple-period ordering in GaInP. *Physical Review B* **2001,** *64* (20), 201322.

37. (a) Fetzer, C. M.; Lee, R. T.; Shurtleff, J. K.; Stringfellow, G. B.; Lee, S. M.; Seong, T. Y., The use of a surfactant (Sb) to induce triple period ordering in GaInP. *Applied Physics Letters* **2000,** *76* (11), 1440-1442; (b) Fetzer, C. M.; Lee, R. T.; Jun, S. W.; Stringfellow, G. B.; Lee, S. M.; Seong, T. Y., Sb enhancement of lateral superlattice formation in GaInP. *Applied Physics Letters* **2001,** *78* (10), 1376-1378; (c) Fetzer, C. M.; Lee, R. T.; Chapman, D. C.; Stringfellow, G. B., Spectroscopic study of surfactant enhanced organometallic vapor phase epitaxy growth of GaInP. *Journal of Applied Physics* **2001,** *90* (2), 1040-1046.

38. Wixom, R. R.; Rieth, L. W.; Stringfellow, G. B., Te surfactant effects on the morphology of patterned (0 0 1) GaAs homoepitaxy. *Journal of Crystal Growth* **2004,** *269* (2–4), 276-283.

39. (a) Niu, X.; Stringfellow, G. B.; Liu, F., Phase separation in strained epitaxial InGaN islands. *Applied Physics Letters* **2011,** *99* (21), 213102-3; (b) Niu, X. B.; Stringfellow, G. B.; Liu, F., Nonequilibrium Composition Profiles of Alloy Quantum Dots and their Correlation with the Growth Mode. *Physical Review Letters* **2011,** *107* (7), 076101.